Molecular basis for phosphospecific recognition of histone H3 tails by Survivin paralogues at inner centromeres

Ewa Niedzialkowska[a,b,c], Fangwei Wang[d], Przemyslaw J. Porebski[b], Wladek Minor[b], Jonathan M. G. Higgins[d], and P. Todd Stukenberg[a]

[a]Department of Biochemistry and Molecular Genetics and [b]Department of Molecular Physiology and Biological Physics, University of Virginia School of Medicine, Charlottesville, VA 22908; [c]Department of Cell Biology, Faculty of Biochemistry, Biophysics and Biotechnology, Jagiellonian University, 30-387 Cracow, Poland; [d]Division of Rheumatology, Immunology and Allergy, Brigham and Women's Hospital, Harvard Medical School, Boston, MA 02115

ABSTRACT **Survivin, a subunit of the chromosome passenger complex (CPC), binds the N-terminal tail of histone H3, which is phosphorylated on T3 by Haspin kinase, and localizes the complex to the inner centromeres. We used x-ray crystallography to determine the residues of Survivin that are important in binding phosphomodified histone H3. Mutation of amino acids that interact with the histone N-terminus lowered in vitro tail binding affinity and reduced CPC recruitment to the inner centromere in cells, validating our solved structures. Phylogenetic analysis shows that nonmammalian vertebrates have two Survivin paralogues, which we name class A and B. A distinguishing feature of these paralogues is an H-to-R change in an amino acid that interacts with the histone T3 phosphate. The binding to histone tails of the human class A paralogue, which has a histidine at this position, is sensitive to changes around physiological pH, whereas *Xenopus* Survivin class B is less so. Our data demonstrate that Survivin paralogues have different characteristics of phosphospecific binding to threonine-3 of histone H3, providing new insight into the biology of the inner centromere.**

Monitoring Editor
Kerry S. Bloom
University of North Carolina

Received: Nov 7, 2011
Revised: Feb 16, 2012
Accepted: Feb 17, 2012

INTRODUCTION

Before chromosomes are segregated during anaphase, microtubules of the mitotic spindle must attach to each mitotic chromosome in a bipolar manner (Tanaka *et al.*, 2002). The chromosome passenger complex (CPC) releases kinetochore microtubule attachments that do not generate proper pulling forces, generating a spindle checkpoint signal that prevents anaphase onset until each chromosome is properly attached (Biggins *et al.*, 1999; Biggins and Murray, 2001; Kallio *et al.*, 2002; Tanaka *et al.*, 2002). It is unclear how the CPC, which is predominantly localized to the inner centromere, regulates kinetochores, which can be hundreds of angstroms away. The CPC contains Survivin (baculoviral inhibitor of apoptosis protein [IAP] repeat-containing protein 5), INCENP, Dasra/Borealin, and the Aurora B kinase (Cooke *et al.*, 1987; Adams *et al.*, 2000; Bolton *et al.*, 2002; Romano *et al.*, 2003; Gassmann *et al.*, 2004; Sampath *et al.*, 2004). The Survivin and Dasra/Borealin proteins bind the N-terminal helical fragment of INCENP, forming a triple coiled-coil (Jeyaprakash *et al.*, 2007), and are required for CPC inner centromere targeting. The Aurora B kinase binds the C-terminus of INCENP (Adams *et al.*, 2000; Bolton *et al.*, 2002). The INCENP subunit has a long coiled-coil motif (Mackay *et al.*, 1993), and therefore tethered CPC may stretch ~400 Å from the inner centromere to allow Aurora B to phosphorylate proteins in the outer kinetochore. Alternatively, soluble gradients of Aurora kinase activity have been recently measured emerging from inner centromeres (Tan and Kapoor, 2011; Wang *et al.*, 2011). This suggests a model by which Aurora B is released from inner centromeres to phosphorylate kinetochore substrates.

This article was published online ahead of print in MBoC in Press (http://www.molbiolcell.org/cgi/doi/10.1091/mbc.E11-11-0904) on February 22, 2012.

Coordinates and structure factors for structures presented in this article were deposited at the Protein Data Bank under the following accession codes: 3UEC, hSurvivin wild-type H3T3ph(1-4); 3UED, hSurvivin wild-type H3T3ph(1-12); 3UEF, hSurvivin wild-type H3T3(1-12); 3UEE, hSurvivin K62A H3T3(1-12); 3UEH, hSurvivin H80A; 3UEG, hSurvivin K62A; and 3UEI, hSurvivin E65A.

Address correspondence to: Jonathan M. G. Higgins (jhiggins@rics.bwh.harvard.edu), P. Todd Stukenberg (pts7h@virginia.edu).

Abbreviations used: BIR, baculoviral inhibitor of apoptosis protein repeat; CPC, chromosomal passenger complex; IAP, inhibitor of apoptosis protein; ITC, isothermal titration calorimetry.

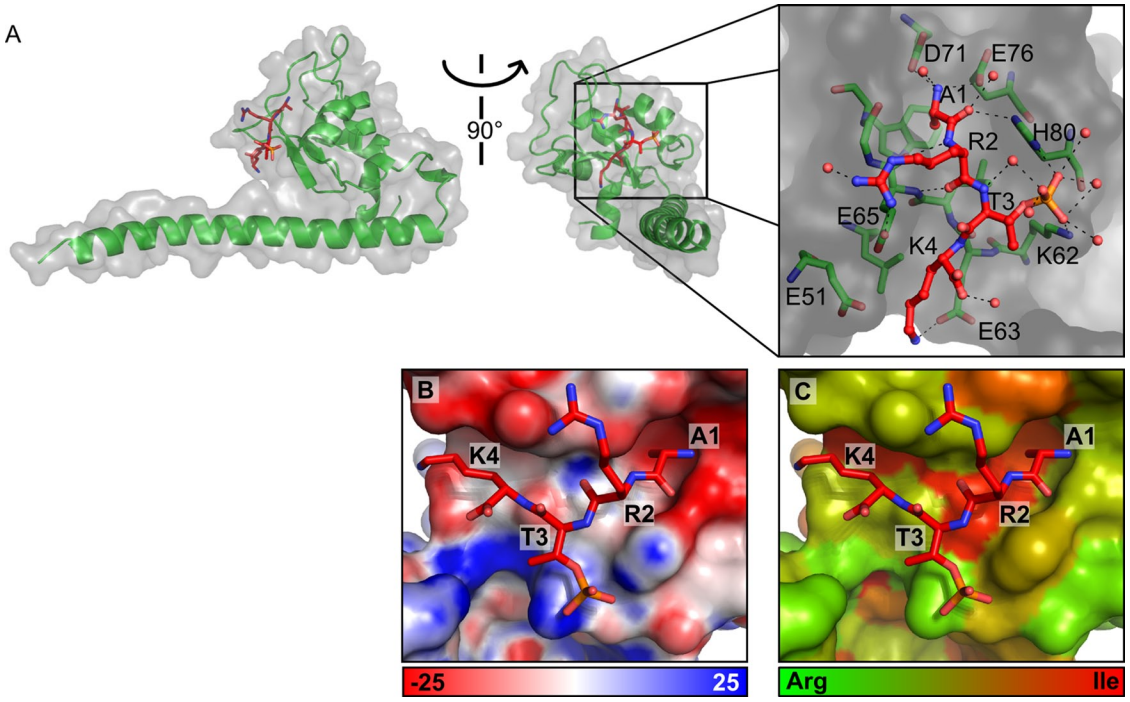

FIGURE 1: Crystal structure of human Survivin with the N-terminal tail of histone H3 phosphorylated on T3. (A) Two orientations of Survivin rotated 90° relative to each other. Survivin is shown in green, and its surface is marked in gray. The peptide molecule is represented with red sticks. Insets show interactions between H3T3ph and Survivin. Inset shows the hydrogen bond network. H3T3ph carbon, nitrogen, oxygen, and phosphorus atoms are shown in dark red, blue, light red, and orange, respectively. Survivin carbon, nitrogen, and oxygen atoms of peptide-binding residues are shown as green, blue, and light red sticks, respectively. Water molecules are presented as light red spheres. Dashes depict probable hydrogen bonds. Marked residues are important in peptide binding. (B) Electrostatic potential on the Survivin surface near the peptide-binding groove. Negatively charged amino acids are marked in red, positively charged ones in blue. (C) Hydrophobicity level of binding pocket for H3T3ph mapped on the Survivin surface. Progressive color change from green to red indicates changes in amino acid hydrophobicity from hydrophilic (arginine [Arg]) to hydrophobic (isoleucine [Ile]).

During mitosis the complex localizes to condensing chromosomes and then concentrates at the inner centromere region that lies between sister kinetochores until anaphase, when it relocates to midzone microtubules and generates gradients of soluble kinase activity to direct cytokinesis (Cooke *et al.*, 1987; Adams *et al.*, 2000; Uren *et al.*, 2000; Gassmann *et al.*, 2004; Fuller *et al.*, 2008). An important step is the localization of the CPC to the inner centromere, which is an event that is directed by the histone code. Histones are the major component of chromatin, and especially their tails are subject to numerous posttranslational modifications, such as phosphorylation, acetylation, or methylation (Berger, 2007; Kouzarides, 2007). Specialized binding proteins often bind these modified tails. Bub1 at kinetochores phosphorylates histone H2A on T120, which recruits Shugoshin proteins that recruit the CPC (Tanno *et al.*, 2010; Tsukahara *et al.*, 2010; Yamagishi *et al.*, 2010). In addition, the Haspin kinase phosphorylates histone H3 on T3 (Dai *et al.*, 2005), which is directly bound by a baculoviral IAP repeat (BIR) domain in the Survivin subunit, providing a binding site for CPC on mitotic centromeres (Kelly *et al.*, 2010; Wang *et al.*, 2010; Yamagishi *et al.*, 2010).

Survivin belongs to the IAP family. These proteins were first described in baculovirus (Crook *et al.*, 1993), as they were able to inhibit defensive host cell death after viral infection. Proteins from this family contain one or more BIRs and are present in a wide variety of organisms. The BIR domain is an ~70–amino acid fold containing a zinc ion coordinated by histidine and cysteine residues (Hinds *et al.*, 1999). Vertebrate Survivins contain a single BIR domain, whereas lower eukaryotic homologues often contain tandem BIR domains.

We used a combination of structural and biophysical methods to describe the molecular basis of the interaction between human Survivin (hSurvivin) and histone H3. By mutational and biological analysis we determined the residues important for interaction between Survivin and histone H3 and crucial for recognition of the phospho-modified T3. Phylogenetic analysis revealed that two Survivin paralogues are present in nonmammalian vertebrates, which, as we demonstrated by biophysical binding studies, differ in apparent specificity to modified T3 of histone H3.

RESULTS

Structure of hSurvivin:H3T3ph complex identifies amino acids crucial for histone tail binding

We determined the crystal structure of human Survivin bound to a four–amino acid peptide ARTphK (H3T3ph(1-4)), which is the sequence of the N-terminus of the histone H3. The complex crystallized in *I222* space group with one monomer in an asymmetric unit and diffracted to 2.18 Å. We were able to determine positions of all four peptide amino acids. The histone H3 tail binds to the BIR domain on a face that is adjacent to the extended C-terminal α-helix that is responsible for interaction with Borealin and INCENP (Figure 1A; Jeyaprakash *et al.*, 2007). The peptide occupies a surface groove formed between the β3 strand, helix D, and the loop in between. The interaction decreased solvent accessible area by 337 Å^2 for Survivin and 434 Å^2 for the H3 tail. We also determined the crystal structure complexed with a 12–amino acid peptide ARTphKQTARKSTG (H3T3ph(1-12)) to 2.7-Å resolution (space group *C2*),

but we were able to unequivocally model only the same four amino acids of the peptide, suggesting that histone H3 recognition is mediated primarily by its four N-terminal amino acids (Supplemental Figure S1).

A small hydrophobic pocket is formed by L64, E76, and W67 that appears too tight to fit large amino acids. The pocket has an acidic environment formed by D71 from a loop region and E76 from helix D that anchor A1 by hydrogen bonds (Figure 1). Survivin residue H80 also contributes to anchoring of the peptide N-terminus by forming a hydrogen bond to the carbonyl of A1 (Figure 1, A and B). A comparison to other proteins from the IAP superfamily showed that recognition of the N-terminal alanine is highly conserved among BIR domain–containing proteins (Supplemental Figure S2A). Not only does histone residue R2 form hydrogen bonds between the carbonyl oxygen and the side chain of E65, but also aliphatic fragments of R2 participate in hydrophobic interactions with the E65 side chain. E65 is not conserved in other BIR domain proteins and provides specificity for the histone H3 interaction.

Survivin binds the phosphothreonine through side chains of H80 and K62 that are hydrogen bonded with adjacent oxygens of the phosphate. Most BIR domains have a W in the position of Survivin's H80 (Supplemental Figure S2A). Replacement of this W with H creates space for and allows hydrogen bonding to the phosphate while preserving the hydrogen bond with A1 (Supplemental Figure S2B). K62 is also not conserved among other BIR domain–containing proteins, which often have a glycine residue at this position.

The K4 side chain of histone H3 forms hydrophobic interactions with both E51 and E63 and may form a weak hydrogen bond with E63. Neither of these amino acids is conserved among other BIR domain–containing proteins.

Structure of hSurvivin wild type and K62A in complex with unphosphorylated H3 peptide

We also solved the crystal structure of the hSurvivin:H3(1-12) complex to 2.45 Å. We observed that the unphosphorylated peptide is bound in the same pocket as the phosphorylated peptide, preserving similar interactions with Survivin, except for those interacting specifically with the phosphate (Figure 2A). The phosphate binding residues do not change conformation substantially in the absence of phosphate.

Because hSurvivin can bind both the phosphorylated and unphosphorylated H3 tail, we generated a set of mutants to examine the relative contributions of particular amino acids to these two binding reactions. We selected H80 and K62, which form hydrogen bonds with the phosphate moiety, for mutational analysis. In addition, we mutated E65, since it appeared to be important for peptide binding regardless of T3 phosphorylation. We crystallized and solved structures of H80A (Protein Data Bank [PDB] ID, 3UEH), K62A (PDB ID, 3UEG), and E65A (PDB ID, 3UEI) and confirmed that the proteins were fully folded, and mutations did not change the conformation of other residues in peptide-binding groove. Cocrystallization of hSurvivin mutants with both peptides was successful only for the K62A mutant. We solved the crystal structure of this mutant in complex with the unmodified H3 peptide. The determined structure shows that there are no striking differences in the H3(1-12) binding by wild type and hSurvivin K62A. However, the resolution of the data from the K62A:H3 crystal does not allow for unambiguous determination of T3 orientation. The side-chain hydroxyl of the unphosphorylated T3 either could be turned away from H80, potentially allowing a hydrophobic interaction between the T3 Cγ and Survivin, or could form a weak hydrogen bond with the H80 side chain (Figure 2B).

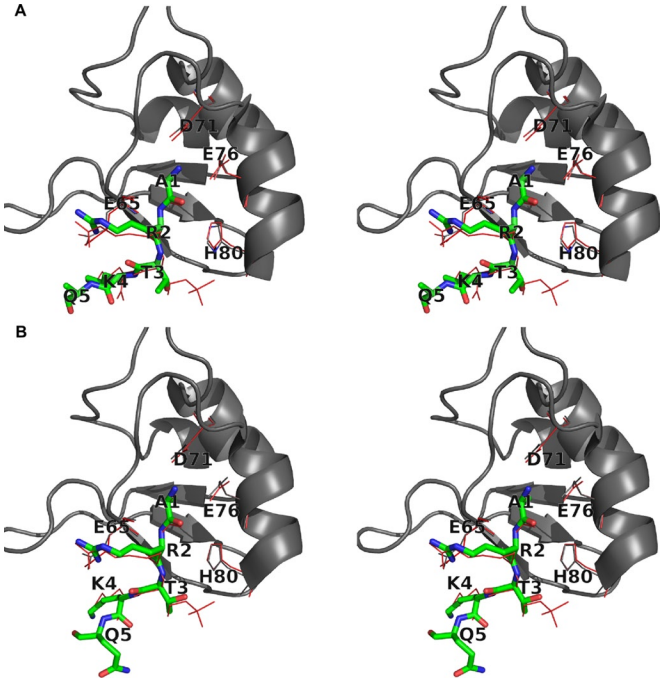

FIGURE 2: Survivin interacts with the unmodified H3 tail in similar way as with H3T3ph. (A) Superposition of the crystal structure of wild-type Survivin with H3T3ph(1-4) (red lines) on the structure of wild-type Survivin (gray; cartoon representation) with H3(1-12) peptide (green in stick representation). For clarity, only D71, D76, H80, E65, and both peptides are shown in line or stick representation. Figures are in stereo representation. (B) Superposition of the crystal structure of wild-type Survivin with H3T3ph(1-4) (red lines) on the structure of K62A Survivin (gray; cartoon representation) with H3(1-12) peptide (green in stick representation). For clarity only, D71, D76, H80, E65, and both peptides are shown in line or stick representation. T3 Oγ can form a weak hydrogen bond with the H80 side chain if present in the modeled orientation. Alternatively, the hydrophobic interactions between T3 Cγ and Survivin may be formed if T3 adopts a different orientation (not shown). Determination of the prevailing orientation of T3 was not possible due to the low quality of its corresponding electron density. Figures are in stereo representation.

Mutational analysis of Survivin histone H3–binding region

We measured the dissociation constants (K_d) between hSurvivin K62A, H80A, and E65A mutants and H3T3ph(1-4) and H3(1-4) tail by isothermal titration calorimetry (ITC). We conducted the experiments at pH 7.8 to rule out the influence of histidine side-chain protonation, which, as described in next paragraph, affects binding affinities.

Phosphobinding was undetectable for hSurvivin H80A and K62A mutants using ITC, which verifies the importance of these residues in histone tail recognition (Table 1). In addition, binding of H3T3ph peptide was also defective for Survivin E65A. This is not surprising, since this residue forms hydrophobic interactions, as well as hydrogen bonds with R2, providing a significant contribution to complex formation.

The hSurvivin wild-type structure suggests that the side chain of hSurvivin H80 forms hydrogen bonds with both the phosphate and the carbonyl oxygen of A1. Mutations of either E65 or H80 to alanine abolished detectable binding to unphosphorylated H3 peptides as measured by ITC (Table 1), which is consistent with the observed contacts of these amino acids with unphosphorylated portions of H3. In contrast, Survivin K62A bound the

Protein	N	K_d (μM)	ΔH (cal/mol)	−TΔS (cal/mol)	N	K_d (μM)	ΔH (cal/mol)	−TΔS (cal/mol)
	H3T3ph(1-4)				H3T3(1-4)			
hs wt	1.05 ± 0.05	61.7 ± 8.5	−2120 ± 210	−3640	1.27 ± 0.03	60.6 ± 4	−3160 ± 120	−2600
hs E65A	n/b	n/b	n/b	n/b	n/b	n/b	n/b	n/b
hs H80A	n/b	n/b	n/b	n/b	0.99 ± 0.27	236 ± 50	−3300 ± 1200	−1670
hs K62A	n/b	n/b	n/b	n/b	1.22 ± 0.02	31.3 ± 2.0	−4610 ± 120	−1540
	H3T3ph(1-12)				H3T3(1-12)			
hs wt	1.35 ± 0.06	29.6 ± 5.4	−670 ± 50	−5510	1.56 ± 0.02	21.0 ± 1.8	−1890 ± 40	−4500
hs H80R	1.32 ± 0.05	60.2 ± 5.8	−2750 ± 150	−3010	n/b	n/b	n/b	n/b
xl wt	1.15 ± 0.01	10.6 ± 0.5	−2800 ± 30	−3990	n/b	n/b	n/b	n/b
xl R89H	1.04 ± 0.01	4.8 ± 0.5	−870 ± 15	−6380	1.34 ± 0.02	12.9 ± 1.4	−2720 ± 60	−3960

Measurements were performed in 25°C in a buffer containing 50 mM Tris, pH 7.8, 50 mM NaCl, and 10 mM β-mercaptoethanol. ΔH, enthalpy change; ΔS, entropy change; hs, human Survivin; K_d, dissociation constant; N, stoichiometry; n/b, no binding; T, temperature; wt, wild type; xl, *X. laevis* class B Survivin.

TABLE 1: Thermodynamic parameters of interaction between human or *Xenopus* Survivin and histone H3 peptide.

unphosphorylated peptide well (K_d = 31 ± 2 μM) but could not bind the phosphorylated peptide.

Chromosomal passenger complex shows improper localization in cells expressing hSurvivin mutants

We confirmed that the residues that were important for peptide binding in vitro were also required to localize the CPC to inner centromeres in cells. We generated HeLa cell lines stably expressing either wild-type or mutant Survivin proteins with C-terminal Myc tags, depleted the endogenous protein by small interfering RNA (siRNA) transfection, and performed immunofluorescence with anti-Myc, anti–Aurora B, and anti-centromere (ACA) antibodies. Both wild-type Survivin and Aurora B were localized predominantly to centromeres after depletion and replacement (Figure 3). All mutants were incorporated into the CPC (Supplemental Figure S3A) and allowed localization of the CPC to the central spindle in anaphase (Supplemental Figure S3B). In contrast, exogenous Survivin proteins could not localize efficiently to centromeres if they were mutated at amino acids that interact with A1 or R2 of histone H3 and therefore prevented both phosphorylated and unphosphorylated histone

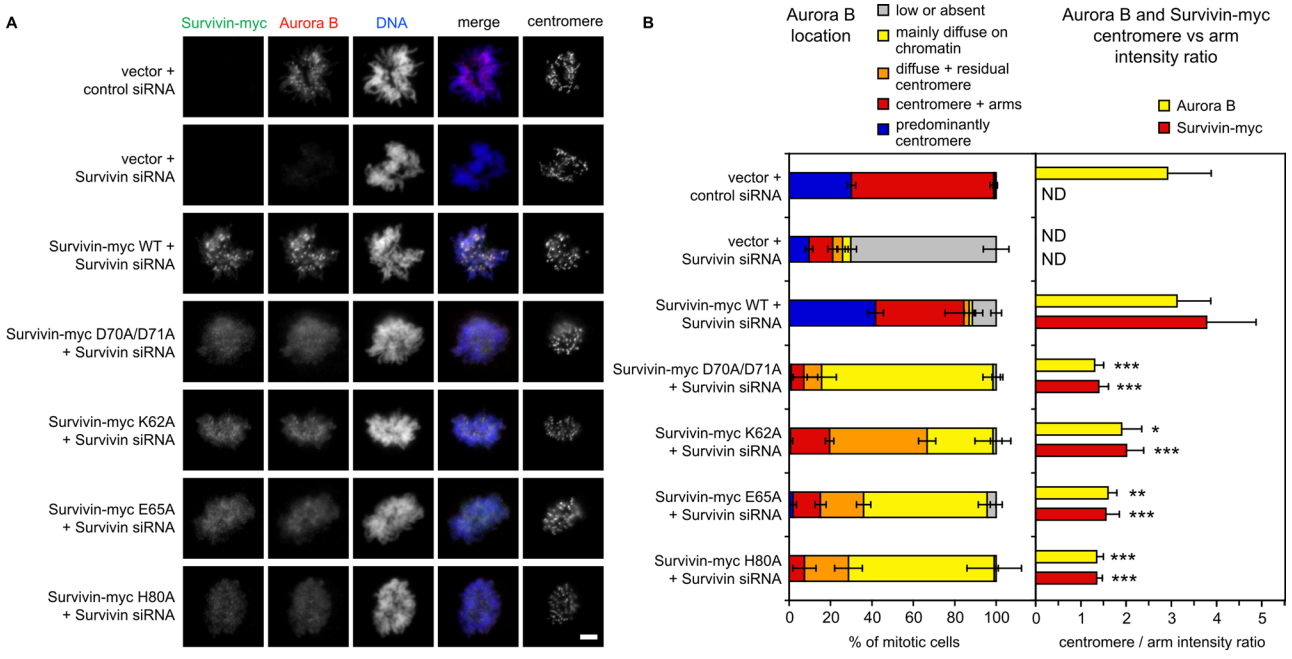

FIGURE 3: Chromosomal passenger complex delocalization in prometaphase in cells expressing mutant Survivin-myc proteins and depleted of endogenous Survivin by siRNA treatment. (A) HeLa cells stably expressing vector alone or Survivin-myc containing the indicated mutations were transfected with siRNA as shown, synchronized by double thymidine block and then released into fresh medium for 12 h, followed by immunostaining with anti–myc epitope antibody (green), anti–Aurora B antibody (red), and ACA. Scale bar, 5 μm. (B) For cells treated as in A, Aurora B localization classified by immunofluorescence microscopy in ~100 cells in each condition is shown on the left. Means ± SD (n = 3). Right, the ratio of centromere to chromosome arm fluorescence intensity for Aurora B and Survivin-myc. Means ± SD (n = 5). ***p < 0.001, **p < 0.01, *p < 0.05 compared with cells expressing Survivin-myc WT by one-way analysis of variance followed by Bonferroni's multiple comparison test. ND, not determined.

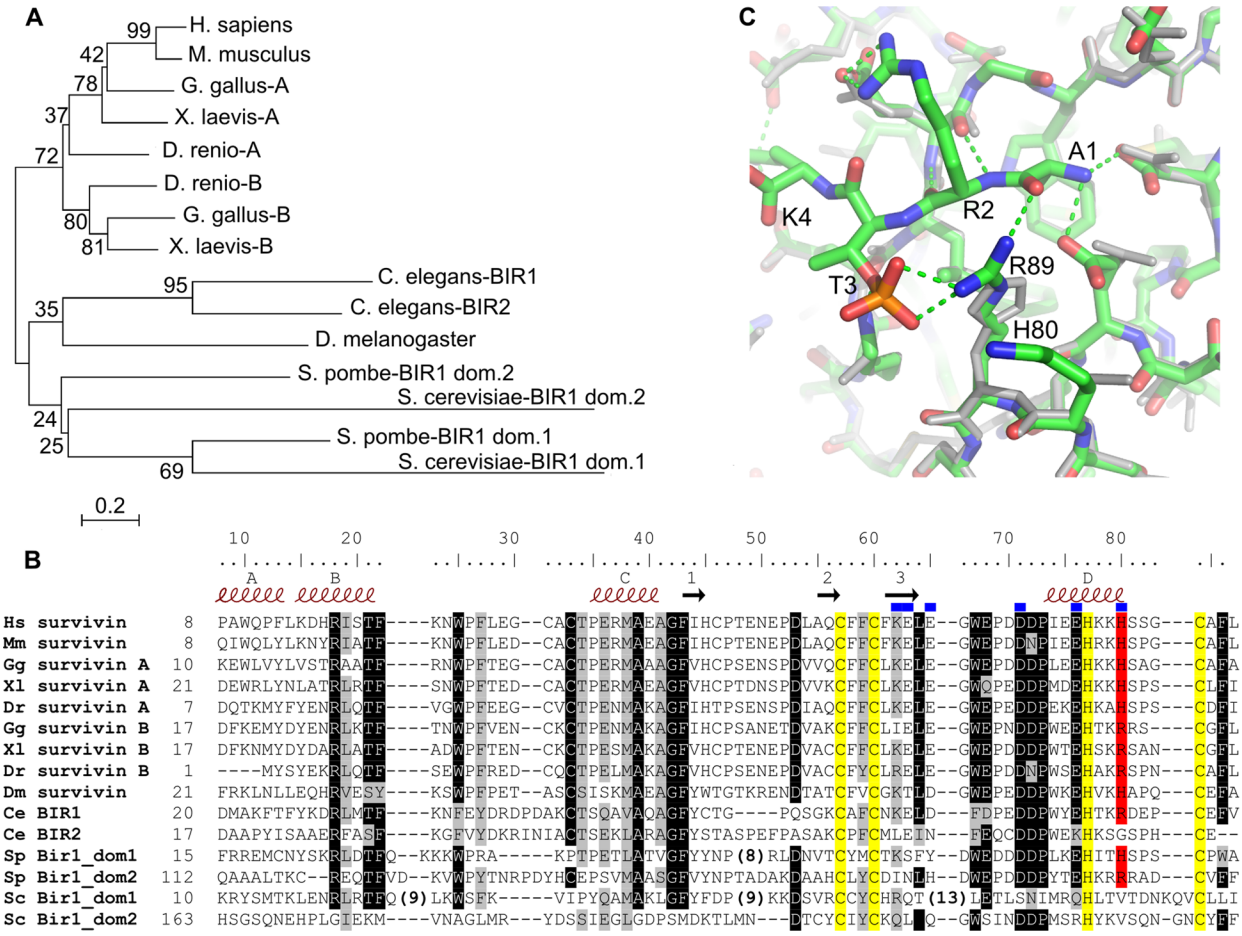

FIGURE 4: Comparison between class A and class B Survivin paralogues. (A) Evolutionary relationships between Survivin proteins. The cladogram of Survivin protein based on sequence alignment in B. The evolution history was deduced using the minimum evolution method. The cladogram is drawn to scale, with branch lengths in the same units as those of the evolutionary distances used to infer the cladogram. Numbers show bootstrap values at the nodes. (B) Sequence alignment of Survivin BIR domains from selected organisms. Residues involved in zinc finger motif formation are marked in yellow. Residues H and R, which distinguish class A and B Survivin, are marked in red. Progressive dark shading indicates identity between 80 and 100%. Numbers on the left side of the alignment indicate the residue from which the alignment begins; numbers on the right are the last residues taken into alignment. Numbers in parentheses are the number of amino acids present in insertions that were removed from alignment. Numbers above the alignment indicate the residue numbering in hSurvivin. Letters from A to D mark helices, and black arrows numbered from 1 to 3 mark β-strands. Residues that form hydrogen bonds with H3 peptide are marked by blue rectangles. N-terminal and C-terminal variable regions and insertions were removed from alignment for clarity. (C) Superposition of the crystal structure of wild-type hSurvivin (gray) and homology model of xSurvivin-B (green carbon atoms). Mutated residues in Survivin (human H80 and *Xenopus* R89) and histone H3T3ph(1-4) residues are marked. Green dashes depict probable hydrogen bonds between the homology model of xSurvivin-B and H3T3ph(1-4) peptide.

binding (E65A and a mutant that we previously characterized, D70A/D71A; Wang *et al.*, 2010). Instead, these proteins, together with Aurora B, were found mostly on chromosome arms. One function of Aurora B at inner centromeres is to recruit the microtubule depolymerase MCAK (Andrews *et al.*, 2004; Lan *et al.*, 2004; Ohi *et al.*, 2004). Cells expressing either Survivin E65A or D70A/D71A also poorly recruited MCAK to centromeres (Supplemental Figure S3, C and D). The H80A mutant that loses interactions both with A1 and the T3 phosphate was defective in peptide binding and gave a result similar to E65A in both Aurora B localization and MCAK recruiting activity (Figure 3 and Supplemental Figure S3, C and D).

The K62A mutant that bound the unphosphorylated peptide specifically was deficient at binding centromeres, confirming that phosphobinding is important for CPC targeting (Figure 3). Of interest, however, the K62A mutant allowed weak but consistent residual binding of the CPC to centromeres above that seen with the other mutants (Figure 3).

Two distinct classes of Survivin are present in vertebrates

We performed a phylogenetic analysis of Survivin in a set of model organisms (Figure 4A). We found that mammals have a single Survivin, whereas nonmammalian vertebrates, like *Xenopus laevis* (Song *et al.*, 2003), have two distinct variants. We name the paralogue that includes the mammalian proteins class A, and the other, class B. We looked for class-specific differences in residues important for peptide binding. Of interest, all class A Survivins have H at position 80 (numbered in the human), whereas all class B family members have R at this position (R89 in xSurvivin-B; Figure 4B).

Similarly, in the *Schizosaccharomyces pombe* homologue, which has dual BIR domains, one of the BIR domains has H at the position and the other has R.

To investigate the consequences of the presence of either histidine or arginine in the histone tail–binding region of Survivin, we generated hSurvivin H80R and xSurvivin-B R89H mutant proteins and performed ITC binding assays at pH 7.8. For further discussion, we define Survivin phosphospecificity as a ratio of Survivin affinity toward H3T3ph to affinity toward H3 peptide. Wild-type hSurvivin bound both phosphorylated and unphosphorylated histone tail peptides with comparable affinities, showing a lack of phosphospecificity at pH 7.8 (Table 1). In contrast the wild-type *Xenopus* Survivin-B showed distinct phosphospecificity, and binding could only be detected to the H3T3ph-modified peptide. Survivin's behavior was reversed by mutations in the H/R residue that binds the phosphate (H80/R89). Although it displayed lower affinity for H3T3ph(1-12) peptide, hSurvivin H80R gained phosphospecificity. Moreover, xSurvivin-B R89H lost phosphospecificity, even though the affinity for H3T3ph(1-12) peptide was increased twofold in comparison to wild-type xSurvivin-B protein (Table 1). We conclude that the presence of H or R in the phosphobinding pocket is an important determinant of binding characteristics, and we propose that this difference distinguishes the two Survivin paralogues.

Biochemical differences between class A and class B Survivins

Because the pKa of histidine is around neutral, we hypothesized that the binding of class A Survivins to histone tails might be responsive to pH. To test this, we investigated the effect of pH and temperature on the Survivin–histone tail interaction. ITC binding assays were carried out within the pH range 6.8–8.2 at 25°C. In general, hSurvivin bound phosphorylated histone tails with higher affinity at lower pH. hSurvivin phosphospecificity for histone tails is pH sensitive within the range of screened pH. At pH 6.8, binding to H3T3ph(1-12) peptide is eightfold better than to unmodified H3(1-12). H3T3ph binding affinity decreases when the pH increases, and the rate of this change is faster than for H3(1-12). At pH 7.8, hSurvivin loses phosphospecificity, having similar binding affinities for both peptides, and at pH 8.2, it binds unphosphorylated peptide preferentially (Figure 5, A and B). In addition, we observed about threefold-better binding to H3T3ph than H3 peptides, using differential scanning fluorimetry assays (Niesen *et al.*, 2007) at pH 7.5 (K_d = 52 ± 8 μM phosphorylated vs. 171±40 μM unphosphorylated peptide; Supplemental Figure S4), and in a parallel study twofold-better binding was observed using ITC at pH 7.5 (Du *et al.*, 2012). We compared binding at 25 and 37°C at pH 6.8, but no major effect of temperature on hSurvivin phosphospecificity was noted. In contrast, xSurvivin-B binds H3T3ph peptides with similar affinity (K_d around 6 μM) within 6.8–7.8 pH range. XSurvivin-B was phosphospecific at all measured pH values (Figure 5, A and B, and Table 2). However, in contrast to hSurvivin, the phosphospecificity increased with pH, which was caused by decrease in affinity toward the unphosphorylated peptide, a finding for which we do not have a good explanation.

Our mutational analysis of the histone tail–binding region showed that both xSurvivin-B and the hSurvivin H80R mutant bind H3T3ph and H3T3 peptides with lower affinity than wild-type hSurvivin. Moreover, xSurvivin-B R89H binds both forms of the histone tail with higher affinity than wild-type xSurvivin-B or hSurvivin-A. These binding experiments, performed on both Survivin classes, suggest that histidine can contribute more strongly than arginine to formation of a histone tail–binding pocket.

DISCUSSION

We determined the structure of hSurvivin bound to modified and unmodified histone H3 peptide. Our crystal structures reveal residues important for peptide binding (E65, D71, and H80) and recognition of phosphorylation on T3 of histone H3 (H80 and K62). E65, H80, and K62 are not conserved in other BIR domains, and mutational analysis of these residues confirmed their importance for H3 peptide binding, both in vitro and for proper centromeric localization of the CPC in cells.

We found that many vertebrates have two Survivin paralogues and that they differ in their interactions with histone H3 tails. We identified an amino acid that contacts the phosphate that can distinguish these classes. The Survivin homologue in *S. pombe* has dual BIR domains, and one domain has H and the other has R at the

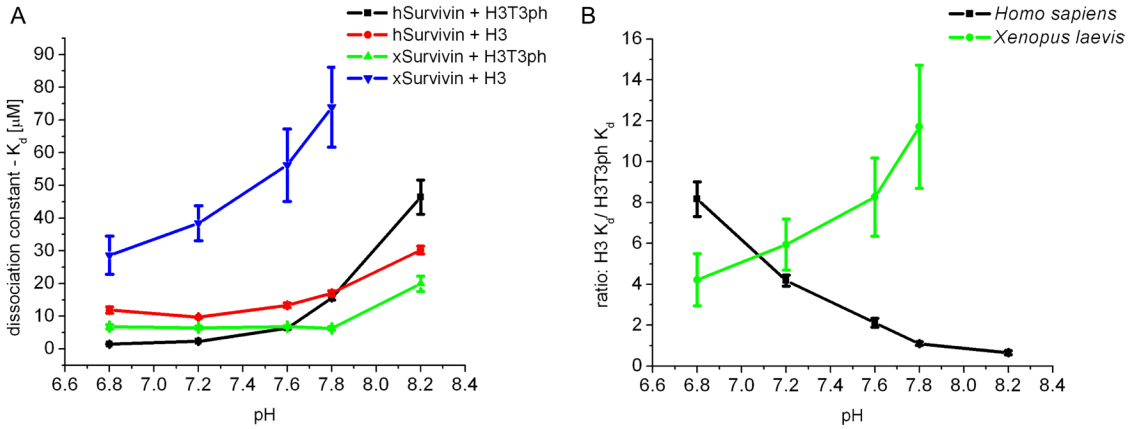

FIGURE 5: pH dependence of histone-binding affinity and phosphospecificity of class A and class B Survivins. (A) Differences in affinity of Survivin class A and class B toward H3T3ph(1-12) and H3(1-12) peptides depending on pH changes. Survivin class A is represented by hSurvivin, and Survivin class B is represented by xSurvivin. (B) Differences in phosphospecificity between Survivin class A (*Homo sapiens*) and class B (*X. laevis*) within pH range 6.8–8.2. Phosphospecificity is displayed as a ratio of the Survivin affinity to H3T3ph peptide to the affinity to H3 peptide, $(1/K_d\text{H3T3ph})/(1/K_d\text{H3})$.

Protein	N	K_d (μM)	ΔH (cal/mol)	−TΔS (cal/mol)	pH	N	K_d (μM)	ΔH (cal/mol)	−TΔS (cal/mol)
	H3T3ph(1-12)					H3(1-12)			
hs wt	1.13 ± 0.001	1.45 ± 0.03	−5640 ± 20	−2320	6.8	1.26 ± 0.01	11.8 ± 1.0	−2490 ± 60	−4220
hs wt	1.03 ± 0.002	2.31 ± 0.08	− 4880 ± 30	−2800	7.2	1.29 ± 0.01	9.67 ± 0.31	−2790 ± 20	−4040
hs wt	1.12 ± 0.01	6.29 ± 0.31	−4650 ± 50	−2440	7.6	1.36 ± 0.01	13.3 ± 0.7	−3210 ± 50	−3430
hs wt	1.20 ± 0.01	15.6 ± 0.6	−4720 ± 60	−1830	7.8	1.33 ± 0.01	17.1±0.8	−3320 ± 50	−3180
hs wt	1.23 ± 0.02	46.4 ± 5.2	−4130 ± 220	−1780	8.2	1.32 ± 0.01	30.2 ± 1.2	−3430 ± 50	−2730
hs H80R	1.02 ± 0.01	26.3 ± 2.0	−3030 ± 90	−3210	6.8	n/b	n/b	n/b	n/b
hs wt 37°C	1.01 ± 0.002	2.85 ± 0.06	−6850 ± 20	−706	6.8	1.37 ± 0.04	21.4 ± 3.2	−4320 ± 230	−2080
xl wt	0.82 ± 0.01	6.79 ± 0.67	−3050 ± 80	−3990	6.8	0.97±0.03	28.7 ± 5.9	−1840 ± 150	−4350
xl wt	1.06 ± 0.01	6.47 ± 0.47	−3080 ± 50	−4000	7.2	1.24 ± 0.03	38.4 ± 5.3	−2260 ± 140	−3760
xl wt	1.21 ± 0.004	6.80 ± 0.24	−3580 ± 30	−3460	7.6	1.31 ± 0.05	56.2 ± 11.1	−2730 ± 270	−3060
xl wt	0.94 ± 0.01	6.31 ± 0.58	−3900 ± 80	−3190	7.8	1.04 ± 0.02	73.9 ± 12.2	− 3680 ± 380	−1950
xl wt	1.04 ± 0.02	19.9 ± 2.4	−4480 ± 210	−1990	8.2	n/b	n/b	n/b	n/b
xl R89H	1.09 ± 0.004	1.01 ± 0.09	−4570 ± 40	−3600	6.8	1.15 ± 0.01	5.21 ± 0.39	−2690 ± 40	−4510

Unless stated (hs wt 37°C), measurements were performed at 25°C in a triple-component buffer containing HEPES:citric acid:Ches and 10 mM β-mercaptoethanol. ΔH, enthalpy change; ΔS, entropy change; hs, human Survivin; K_d, dissociation constant; N, stoichiometry; n/b, no binding; T, temperature; wt, wild type; xl, *X. laevis* class B Survivin.

TABLE 2: Thermodynamic parameters of interaction between human or *Xenopus* Survivin and histone H3 peptide within pH range 6.8–8.2.

phosphate-binding position, which suggests the evolutionary conservation of the importance of the two classes working together to properly localize the CPC.

In this study we showed that interaction between hSurvivin and the phosphorylated tail of histone H3 is pH sensitive and enhanced at pH 6.8. The likely reason for this pH dependence is protonation of the side chain of H80. In the investigated pH range, the phosphate of the phosphothreonine is most probably unprotonated (Hoffmann *et al.*, 1994) and is likely to act as a hydrogen bond acceptor, as is the carbonyl oxygen of A1. In our structure we observed that the two nitrogen atoms in the imidazole ring of H80 are in positions suitable for forming hydrogen bonds with the A1 carbonyl oxygen and the T3 phosphate (Figure 1). Only a histidine carrying protons on both nitrogens of its side chain can act as a donor for two hydrogen bonds in this environment. This form of H80 will also be positively charged and favor an interaction with the negatively charged phosphate moiety. Thus we propose that lower pH will facilitate protonation of H80 to allow proper binding of phosphothreonine and that the absence of a charged histidine at higher pH may account for the pH sensitivity of hSurvivin in phosphospecific binding of the H3 tail. This also explains the less-pH-dependent phosphopeptide binding of xSurvivin-B, as the charge of R89 is not expected to be affected by pH in the investigated range.

Under certain conditions both hSurvivin and xSurvivin-B R89H bind phosphorylated histone tails better than the corresponding proteins with arginine. However, the cost of better binding appears to be pH sensitivity, since, at pH 7.8, hSurvivin and xSurvivin-B R89H have decreased phosphospecificity. In contrast, xSurvivin-B and hSurvivin H80R bind phosphorylated histone tails with lower affinity than the corresponding proteins with a histidine in the binding region, but they retain phosphospecificity across the investigated pH range. We believe that this observed difference in pH dependence may be an important class A versus B distinction. Although it is interesting to speculate that binding of the class A Survivins to inner centromeres might be sensitive to local changes of pH, another explanation might be that intracellular pH differs in different organisms or cell types. Most measurements in *Xenopus* eggs yield a pH of 7.7 (Webb and Nuccitelli, 1981), whereas the intracellular pH of human cells has been measured between pH 7.0 and 7.3 (Roos and Boron, 1981), with more recent values around pH 7.2 (Llopis *et al.*, 1998). However, the local chromatin pH value remains unknown. Thus, in species that have two Survivin paralogues, the relative amounts of each may reflect pH differences in different cell types.

We do not fully understand why Survivin with an arginine in the binding pocket would bind H3 peptides with lower affinities than Survivin with a histidine. We speculate that, in the nonbound state, arginine in class B Survivins blocks the peptide binding cleft because its longer side chain allows it to form hydrogen bonds and electrostatic interactions with E85 on one side of the pocket and electrostatic interactions with E74 on the other side (see homology model in Supplemental Figure S5, residue numbering for xSurvivin-B). Therefore the side chain of R89 must break these interactions and change its conformation to accommodate the peptide. It is possible that the interaction with the negatively charged phosphate would facilitate this conformational change and favor formation of intermolecular hydrogen bonds with the phosphorylated peptide. The intramolecular interactions of R89 in the tail-binding pocket may be too strong to be broken by interaction with T3 of an unmodified histone tail, which could explain why class B Survivins poorly bind unphosphorylated peptides. In the case of hSurvivin, the histidine in the corresponding position does not form intramolecular hydrogen bonds, and thus its observed better affinity may result from formation of new hydrogen bonds upon binding of phosphorylated peptide without breaking prior intramolecular bonds.

During preparation of this article, two reports were published that also describe the interaction between hSurvivin and histone H3T3ph (Jeyaprakash *et al.*, 2011; Du *et al.*, 2012). The structures presented by both groups have the same crystal forms as ours, and the authors

denote the same histone tail–binding groove and point to the same amino acids that participate in the interaction between Survivin and the phosphorylated N-terminal peptide from histone H3. Of interest, Du *et al.* (2012) also describe the binding between Survivin and a Smac/DIABLO N-terminal fragment, suggesting a common mechanism for the dual role for Survivin in mitosis and apoptosis.

The apparent lack of phosphospecificity of human Survivin at pH 7.8, as well as the modest phosphospecificity at pH 7.5, pointed out in a recent article (Du *et al.*, 2012) was initially a surprise. This brought into doubt that Haspin phosphorylation of histone H3 is critical for Survivin binding. The solution to this conundrum is likely to be the pH dependence, since at pH 6.8 human Survivin bound phosphorylated peptides with almost eightfold higher affinity than unmodified peptides. A second minor difference between the studies concerns the properties of the Survivin K62A mutant. Du *et al.* (2012) reported that this mutant loses the modest phosphospecificity they detect for wild-type Survivin, but that it still binds H3T3ph peptides. In contrast, we have been unable to detect any binding of Survivin K62A to H3T3ph-modified peptides using the structural and biochemical analysis described earlier, though in both articles this mutant retains binding affinity for unmodified tails in vitro. We find that Survivin K62A is strongly compromised in localization to centromeres in cells, attesting to the likely importance of phosphospecificity in vivo.

A number of recent publications have provided important insight into the pathways that target the CPC to inner centromeres. Together they suggest that the CPC is targeted by at least two mechanisms that emanate from the histone codes of the inner centromere. First, the CPC indirectly reads the histone code through Shugoshin. Recruitment of Shugoshin to centromeres requires phosphorylation of histone H2A on T120 by the Bub1 kinase (Yamagishi *et al.*, 2010), although whether the interaction is direct or indirect requires further investigation. Shugoshin from *S. pombe* binds the CPC after CDK1 phosphorylation (Tsukahara *et al.*, 2010), and it has been proposed that these mechanisms are conserved in vertebrates (Yamagishi *et al.*, 2010). Moreover, it has been recently suggested, based on in vitro studies, that the N-terminus of Sgo1 could directly bind Survivin in the same pocket that we describe (Jeyaprakash *et al.*, 2011). Second, the CPC also directly binds histone H3 tails in the inner centromere after they are phosphorylated by Haspin kinase. It will also be important in the future to understand on the molecular level how Shugoshin is recruited to histone H2A and binds the CPC.

MATERIALS AND METHODS

Protein purification

Recombinant human Survivin wild-type and mutated proteins were overexpressed in *Escherichia coli* strain BL21-CodonPlus (DE3) RIL (Stratagene, Santa Clara, CA) using the pHIS8 expression vector including N-terminal octahistidine tag with thrombin cleavage site. Amino acid mutations were introduced using QuikChange Site-Directed Mutagenesis Kit (Stratagene). Bacteria were induced at OD 2.0 with 0.6 mM isopropyl-β-D-thiogalactoside followed by adding 80 μM $ZnCl_2$ per 1 l of Terrific Broth (TB) medium. Cells were incubated with shaking for 16 h at 18°C. Cells were harvested, and pellets were suspended in buffer A (50 mM Tris, pH 7.9, 500 mM NaCl, 5% glycerol, 10 mM β-mercaptoethanol) containing 10 mM imidazole and Complete Inhibitor Protease Cocktail (Roche, Indianapolis, IN). After sonication, lysates were ultracentrifuged at 30,000 rpm for 40 min at 4°C. The supernatants were incubated with Ni^{2+} resin at 4°C. Beads were washed in buffer A containing 25 mM imidazole, and proteins were eluted with buffer A containing 250 mM Imidazole. The octahistidine tag was removed by thrombin digestion during dialysis in buffer (50 mM Tris, pH 8.0, 500 mM NaCl, and 10 mM β-mercaptoethanol). Protein was loaded on Superdex200, and desired fractions were dialyzed to 5 mM 4-(2-hydroxyethyl)-1-piperazineethanesulfonic acid (HEPES)-Na, pH 7.5, and 10 mM β-mercaptoethanol buffer. Recombinant *Xenopus* Survivin wild-type and mutated proteins with uncleavable C-terminal hexahistidine tag were overexpressed in *E. coli* strain BL21-CodonPlus (DE3) RIL (Stratagene) using the pET28a expression vector and purified following the same protocol as for human Survivin, except for proteolytic digestion.

Crystallization, data collection, structure refinement, and analysis

Crystals of hSurvivin were grown in hanging drops at 16°C using EasyXtal Tools crystallization plates. The drop was composed of 1 μl of protein mixed with 1 μl of mother liquor solution. Peptides ARTphK, ARTK, ARTphKQTARKSTG, and ARTKQTARKSTG (GenScript, Piscataway, NJ) were used in crystallization experiments. Before flash cooling in liquid nitrogen, crystals were cryoprotected in crystallization buffer containing 33% ethylene glycol. Crystallization conditions are presented in Supplemental Table S1. Structure of hSurvivin with H3T3ph(1-4) was obtained by using a single-wavelength anomalous dispersion technique using bound Zn^{2+} ions. Structures of hSurvivin wild type with H3T3ph(1-12), hSurvivin with H3T3(1-12) peptide, and hSurvivin K62A with H3T3(1-12) peptide were solved by molecular replacement using wild-type structure as a model. Data collection was performed on 19ID or 21ID beamline at Argonne National Laboratory (Argonne, IL). Data processing and model building were done with HKL-3000 (Minor *et al.*, 2006) integrated with SHELXD and SHELXE (Sheldrick, 2008), MLPHARE (Otwinowski, 1991), DM (Cowtan and Main, 1993), and ARP/wARP (Perrakis *et al.*, 1999). Molecular replacement was performed using HKL-3000 and MOLREP (Vagin and Teplyakov, 1997). The resulting model was further refined with REFMAC5 (Murshudov *et al.*, 1997) and COOT (Emsley *et al.*, 2010). Structure was validated using MOLPROBITY (Chen *et al.*, 2010) and ADIT (Yang *et al.*, 2004) tools. Refinement statistics are presented in Supplemental Table S2. Figures were prepared using PyMOL (www.pymol.org). Electrostatic potential was calculated for the hSurvivin H3T3ph(1-4) model without the peptide using APBS (Baker *et al.*, 2001). Preparation of the model was done with PDB2PQR (Dolinsky *et al.*, 2007).

Isothermal titration calorimetry

Binding experiments were performed in buffer (50 mM Tris, pH 7.5, 50 mM NaCl, and 10 mM β-mercaptoethanol) using an iTC200 isothermal titration calorimeter (MicroCal, Northampton, MA). First titration was carried out using 0.5 μl of 1.2 mM peptide, followed by fifteen 2.5-μl injections applied 180 s apart. Protein concentration was 0.1 mM. Titration experiments were conducted at 25 or 37°C. A binding isothermal fit was done with Origin software using a single-binding-site model with stoichiometry, ΔH (enthalpy change), and K_a as variable. The citric acid-Ches-HEPES buffer system was used to screen pH within the range 6.8–7.2. Buffers were prepared as described (Newman, 2004) and adjusted to desired pH. Single data sets were fitted to a single-site ITC binding model using a baseline offset parameter to account for heats of dilution.

Cell lines and transfection

HeLa cell lines stably expressing human Survivin and its mutants were established by transfection with pEF6-Survivin-myc-His (Yixian Zheng, Carnegie Institution of Washington, Washington, DC; Vong *et al.*, 2005) and selection in 2 μg/ml blasticidin (Wang *et al.*, 2010). Survivin siRNA targeting the endogenous 3′ untranslated region from Applied Biosystems/Ambion (Austin, TX; s1458) was introduced

into cells with Oligofectamine (Invitrogen, Carlsbad, CA). Cells were typically analyzed 48 h after siRNA transfection. Where indicated, cells were synchronized at G1/S by treatment with 2 mM thymidine (Calbiochem, La Jolla, CA). In some cases, cells were additionally arrested in prometaphase by treatment with 200 ng/ml nocodazole (Sigma-Aldrich, St. Louis, MO).

Fluorescence microscopy and antibodies

Fluorescence microscopy was carried out as described (Wang *et al.*, 2010). Briefly, cells were fixed with 2% paraformaldehyde in phosphate-buffered saline (PBS) for 10 min, followed by extraction with 0.5% Triton X-100 in PBS for 5 min, at room temperature. After blocking in extraction buffer containing 5% milk, primary and secondary antibodies were diluted in blocking buffer and incubated at room temperature for 1–2 h. Imaging was performed using a 60× Plan Apo (numerical aperture 1.40) oil immersion objective lens and a TE2000-U inverted microscope (Nikon, Melville, NY) equipped with a SPOT-RT charge-coupled device system. Mouse monoclonal antibodies used were to myc-tag (9E10) and sheep antibodies were to Aurora B (Stephen Taylor, University of Manchester, United Kingdom; Ditchfield *et al.*, 2003). Human centromere autoantibodies were from ImmunoVision (Springdale, AZ). Secondary antibodies were donkey anti-sheep immunoglobulin G (IgG)–Alexa 488 (Invitrogen); anti–mouse IgG-Cy3; and anti–human IgG-Cy5 (Jackson ImmunoResearch, West Grove, PA). ImageJ (National Institutes of Health, Bethesda, MD) was used to determine centromere autoantigen intensity within 10 × 4 pixel–ellipses encompassing paired centromere dots. After background correction, the ratio of Aurora B or Survivin-myc to centromere autoantigen intensity was calculated independently for each of 16 centromeres per cell. After background subtraction, the average intensity of Aurora B or Survivin-myc within 10 × 4–pixel ellipses at three locations on chromosome arms was normalized to the average centromere autoantigen intensity in the same cell. The average centromere/arm intensity ratio was then calculated for each cell.

Evolutionary relationships among Survivins

The evolutionary history was inferred using the minimum evolution method (Rzhetsky and Nei, 1992). The optimal tree with the sum of branch length of 9.95 is shown. The percentage of replicate trees in which the associated taxa clustered together in the bootstrap test (500 replicates) is shown next to the branches (Felsenstein, 1985). The cladogram is drawn to scale, with branch lengths in the same units as those of the evolutionary distances used to infer the phylogenetic tree. The evolutionary distances were computed using the JTT matrix-based method (Jones *et al.*, 1992) and are in the units of the number of amino acid substitutions per site. The ME tree was searched using the close-neighbor-interchange algorithm (Nei and Kumar, 2000) at a search level of 0. The neighbor-joining algorithm (Saitou and Nei, 1987) was used to generate the initial tree. The analysis involved 15 amino acid sequences. All ambiguous positions were removed for each sequence pair. There were a total of 133 positions in the final data set. Evolutionary analyses were conducted in MEGA5 (Tamura *et al.*, 2011).

Sequence alignment of Survivin's BIR domain and homology modeling of *Xenopus* Survivin class B

Sequence alignment of Survivin's BIR domain was performed with CLUSTALW2 at EBI server using default parameters and then refined manually The homology model of *Xenopus* Survivin class B was generated on the basis of the alignment presented in Figure 4C using the SWISS-MODEL server (Arnold *et al.*, 2006) with the PDB:2QFA (Jeyaprakash *et al.*, 2007) model as a template. H3T3ph peptide was introduced from the PDB:3UEC model, and the geometry of the models was optimized in the OPLS-AA force field using GROMACS (Van Der Spoel *et al.*, 2005). Parametrization of unprotonated phosphothreonine was derived from previous studies (Homeyer *et al.*, 2006).

ACKNOWLEDGMENTS

We thank M. Chruszcz for his valuable discussions. This work was supported by National Institutes of Health Grants R01GM063045 and R01GM081576 to P.T.S., R01GM074210 to J.M.G.H., and GM053163 to W.M., by a Scholar Award from the Leukemia and Lymphoma Society to J.M.G.H., and in part by a gift provided to the University of Virginia by Altria USA to E.N. and P.T.S. The review and approval process was overseen by an External Advisory Committee without any affiliation with the University, Altria USA, or any other tobacco company. Funding for this project was based on independent intramural and extramural reviews. We thank Andrzej Joachimiak, Keith Brister, and the Structural Biology Center/Life Sciences Collaborative Access (LS-CAT) Team at the Argonne Advanced Photon Source for their assistance during synchrotron x-ray data collection. The results are derived from work performed at Argonne National Laboratory at the Structural Biology Center and LS-CAT Sector 21 of the Advanced Photon Source. Use of the Advanced Photon Source was supported by the U.S. Department of Energy, Office of Science, Office of Basic Energy Sciences, under Contract No. DE-AC02-06CH11357. Use of the LS-CAT Sector 21 was supported by the Michigan Economic Development Corporation and the Michigan Technology Tri-Corridor for the support of this research program (Grant 085P1000817).

REFERENCES

Adams RR, Wheatley SP, Gouldsworthy AM, Kandels-Lewis SE, Carmena M, Smythe C, Gerloff DL, Earnshaw WC (2000). INCENP binds the aurora-related kinase AIRK2 and is required to target it to chromosomes, the central spindle and cleavage furrow. Curr Biol 10, 1075–1078.

Andrews PD, Ovechkina Y, Morrice N, Wagenbach M, Duncan K, Wordeman L, Swedlow JR (2004). Aurora B regulates MCAK at the mitotic centromere. Dev Cell 6, 253–268.

Arnold K, Bordoli L, Kopp J, Schwede T (2006). The SWISS-MODEL workspace: a Web-based environment for protein structure homology modelling. Bioinformatics 22, 195–201.

Baker NA, Sept D, Joseph S, Holst MJ, McCammon JA (2001). Electrostatics of nanosystems: application to microtubules and the ribosome. Proc Natl Acad Sci USA 98, 10037–10041.

Berger SL (2007). The complex language of chromatin regulation during transcription. Nature 447, 407–412.

Biggins S, Murray AW (2001). The budding yeast protein kinase Ipl1/Aurora allows the absence of tension to activate the spindle checkpoint. Genes Dev 15, 3118–3129.

Biggins S, Severin FF, Bhalla N, Sassoon I, Hyman AA, Murray AW (1999). The conserved protein kinase Ipl1 regulates microtubule binding to kinetochores in budding yeast. Genes Dev 13, 532–544.

Bolton MA, Lan W, Powers SE, McCleland ML, Kuang J, Stukenberg PT (2002). Aurora B kinase exists in a complex with survivin and INCENP and its kinase activity is stimulated by survivin binding and phosphorylation. Mol Biol Cell 13, 3064–3077.

Chen VB, Arendall WB 3rd, Headd JJ, Keedy DA, Immormino RM, Kapral GJ, Murray LW, Richardson JS, Richardson DC (2010). MolProbity: all-atom structure validation for macromolecular crystallography. Acta Crystallogr D Biol Crystallogr 66, 12–21.

Cooke CA, Heck MSH, Earnshaw WC (1987). The inner centromere protein (INCENP) antigens: movement from inner centromere to midbody during mitosis. J Cell Biol 105, 2053–2067.

Cowtan KD, Main P (1993). Improvement of macromolecular electron-density maps by the simultaneous application of real and reciprocal space constraints. Acta Crystallogr D Biol Crystallogr 49, 148–157.

Crook NE, Clem RJ, Miller LK (1993). An apoptosis-inhibiting baculovirus gene with a zinc finger-like motif. J Virol 67, 2168–2174.

Dai J, Sultan S, Taylor SS, Higgins JM (2005). The kinase haspin is required for mitotic histone H3 Thr 3 phosphorylation and normal metaphase chromosome alignment. Genes Dev 19, 472–488.

Ditchfield C, Johnson VL, Tighe A, Ellston R, Haworth C, Johnson T, Mortlock A, Keen N, Taylor SS (2003). Aurora B couples chromosome alignment with anaphase by targeting BubR1, Mad2, and Cenp-E to kinetochores. J Cell Biol 161, 267–280.

Dolinsky TJ, Czodrowski P, Li H, Nielsen JE, Jensen JH, Klebe G, Baker NA (2007). PDB2PQR: expanding and upgrading automated preparation of biomolecular structures for molecular simulations. Nucleic Acids Res 35, W522–W525.

Du J, Kelly AE, Funabiki H, Patel DJ (2012). Structural basis for recognition of H3T3ph and Smac/DIABLO N-terminal peptides by human Survivin. Structure 20, 185–195.

Emsley P, Lohkamp B, Scott WG, Cowtan K (2010). Features and development of Coot. Acta Crystallogr D Biol Crystallogr 66, 486–501.

Felsenstein J (1985). Confidence-limits on phylogenies—an approach using the bootstrap. Evolution 39, 783–791.

Fuller BG, Lampson MA, Foley EA, Rosasco-Nitcher S, Le KV, Tobelmann P, Brautigan DL, Stukenberg PT, Kapoor TM (2008). Midzone activation of Aurora B in anaphase produces an intracellular phosphorylation gradient. Nature 453, 1132–1136.

Gassmann R, Carvalho A, Henzing AJ, Ruchaud S, Hudson DF, Honda R, Nigg EA, Gerloff DL, Earnshaw WC (2004). Borealin: a novel chromosomal passenger required for stability of the bipolar mitotic spindle. J Cell Biol 166, 179–191.

Hinds MG, Norton RS, Vaux DL, Day CL (1999). Solution structure of a baculoviral inhibitor of apoptosis (IAP) repeat. Nature Struct Biol 6, 648–651.

Hoffmann R, Reichert I, Wachs WO, Zeppezauer M, Kalbitzer HR (1994). 1H and 31P NMR spectroscopy of phosphorylated model peptides. Int J Peptide Protein Res 44, 193–198.

Homeyer N, Horn AH, Lanig H, Sticht H (2006). AMBER force-field parameters for phosphorylated amino acids in different protonation states: phosphoserine, phosphothreonine, phosphotyrosine, and phosphohistidine. J Mol Model 12, 281–289.

Jeyaprakash AA, Basquin C, Jayachandran U, Conti E (2011). Structural basis for the recognition of phosphorylated histone H3 by the survivin subunit of the chromosomal passenger complex. Structure 19, 1625–1634.

Jeyaprakash AA, Klein UR, Lindner D, Ebert J, Nigg EA, Conti E (2007). Structure of a Survivin-Borealin-INCENP core complex reveals how chromosomal passengers travel together. Cell 131, 271–285.

Jones DT, Taylor WR, Thornton JM (1992). The rapid generation of mutation data matrices from protein sequences. Comput Appl Biosci 8, 275–282.

Kallio MJ, McCleland ML, Stukenberg PT, Gorbsky GJ (2002). Inhibition of aurora B kinase blocks chromosome segregation, overrides the spindle checkpoint, and perturbs microtubule dynamics in mitosis. Curr Biol 12, 900–905.

Kelly AE, Ghenoiu C, Xue JZ, Zierhut C, Kimura H, Funabiki H (2010). Survivin reads phosphorylated histone H3 threonine 3 to activate the mitotic kinase Aurora B. Science 330, 235–239.

Kouzarides T (2007). Chromatin modifications and their function. Cell 128, 693–705.

Lan W, Zhang X, Kline-Smith SL, Rosasco SE, Barrett-Wilt GA, Shabanowitz J, Hunt DF, Walczak CE, Stukenberg PT (2004). Aurora B phosphorylates centromeric MCAK and regulates its localization and microtubule depolymerization activity. Curr Biol 14, 273–286.

Llopis J, McCaffery JM, Miyawaki A, Farquhar MG, Tsien RY (1998). Measurement of cytosolic, mitochondrial, and Golgi pH in single living cells with green fluorescent proteins. Proc Natl Acad Sci USA 95, 6803–6808.

Mackay AM, Eckley DM, Chue C, Earnshaw WC (1993). Molecular analysis of the INCENPs (inner centromere proteins): separate domains are required for association with microtubules during interphase and with the central spindle during anaphase. J Cell Biol 123, 373–385.

Minor W, Cymborowski M, Otwinowski Z, Chruszcz M (2006). HKL-3000: the integration of data reduction and structure solution—from diffraction images to an initial model in minutes. Acta Crystallogr D Biol Crystallogr 62, 859–866.

Murshudov GN, Vagin AA, Dodson EJ (1997). Refinement of macromolecular structures by the maximum-likelihood method. Acta Crystallogr D Biol Crystallogr 53, 240–255.

Nei M, Kumar S (2000). Molecular Evolution and Phylogenetics, Oxford: Oxford University Press.

Newman J (2004). Novel buffer systems for macromolecular crystallization. Acta Crystallogr D Biol Crystallogr 60, 610–612.

Niesen FH, Berglund H, Vedadi M (2007). The use of differential scanning fluorimetry to detect ligand interactions that promote protein stability. Nat Protoc 2, 2212–2221.

Ohi R, Sapra T, Howard J, Mitchison TJ (2004). Differentiation of cytoplasmic and meiotic spindle assembly MCAK functions by Aurora B-dependent phosphorylation. Mol Biol Cell 15, 2895–2906.

Otwinowski Z (1991). Maximum likelihood refinement of heavy atom parameters. In: Isomorphous Replacement and Anomalous Scattering, Daresbury Study Weekend Proceedings, Warrington, United Kingdom: SERC Daresbury Laboratory, 80–85.

Perrakis A, Morris R, Lamzin VS (1999). Automated protein model building combined with iterative structure refinement. Nat Struct Biol 6, 458–463.

Romano A, Guse A, Krascenicova I, Schnabel H, Schnabel R, Glotzer M (2003). CSC-1: a subunit of the Aurora B kinase complex that binds to the survivin-like protein BIR-1 and the INCENP-like protein ICP-1. J Cell Biol 161, 229–236.

Roos A, Boron WF (1981). Intracellular pH. Physiol Rev 61, 296–434.

Rzhetsky A, Nei M (1992). A simple method for estimating and testing minimum-evolution trees. Mol Biol Evol 9, 945–967.

Saitou N, Nei M (1987). The neighbor-joining method: a new method for reconstructing phylogenetic trees. Mol Biol Evol 4, 406–425.

Sampath SC, Ohi R, Leismann O, Salic A, Pozniakovski A, Funabiki H (2004). The chromosomal passenger complex is required for chromatin-induced microtubule stabilization and spindle assembly. Cell 118, 187–202.

Sheldrick GM (2008). A short history of SHELX. Acta Crystallogr A 64, 112–122.

Song K, Kim TM, Kim HJ, Kim JW, Kim HH, Kwon HB, Kim WS, Choi HS (2003). Molecular cloning and characterization of a novel inhibitor of apoptosis protein from *Xenopus laevis*. Biochem Biophys Res Commun 301, 236–242.

Tamura K, Peterson D, Peterson N, Stecher G, Nei M, Kumar S (2011). MEGA5: molecular evolutionary genetics analysis using maximum likelihood, evolutionary distance, and maximum parsimony methods. Mol Biol Evol 28, 2731–2739.

Tan L, Kapoor TM (2011). Examining the dynamics of chromosomal passenger complex (CPC)-dependent phosphorylation during cell division. Proc Natl Acad Sci USA 108, 16675–16680.

Tanaka TU, Rachidi N, Janke C, Pereira G, Galova M, Schiebel E, Stark MJ, Nasmyth K (2002). Evidence that the Ipl1-Sli15 (Aurora kinase-INCENP) complex promotes chromosome bi-orientation by altering kinetochore-spindle pole connections. Cell 108, 317–329.

Tanno Y, Kitajima TS, Honda T, Ando Y, Ishiguro K, Watanabe Y (2010). Phosphorylation of mammalian Sgo2 by Aurora B recruits PP2A and MCAK to centromeres. Genes Dev 24, 2169–2179.

Tsukahara T, Tanno Y, Watanabe Y (2010). Phosphorylation of the CPC by Cdk1 promotes chromosome bi-orientation. Nature 467, 719–723.

Uren AG, Wong L, Pakusch M, Fowler KJ, Burrows FJ, Vaux DL, Choo KH (2000). Survivin and the inner centromere protein INCENP show similar cell- cycle localization and gene knockout phenotype. Curr Biol 10, 1319–1328.

Vagin A, Teplyakov A (1997). MOLREP: an automated program for molecular replacement. J Appl Crystallogr 30, 1022–1025.

Van Der Spoel D, Lindahl E, Hess B, Groenhof G, Mark AE, Berendsen HJ (2005). GROMACS: fast, flexible, and free. J Comput Chem 26, 1701–1718.

Vong QP, Cao K, Li HY, Iglesias PA, Zheng Y (2005). Chromosome alignment and segregation regulated by ubiquitination of survivin. Science 310, 1499–1504.

Wang E, Ballister ER, Lampson MA (2011). Aurora B dynamics at centromeres create a diffusion-based phosphorylation gradient. J Cell Biol 194, 539–549.

Wang F, Dai J, Daum JR, Niedzialkowska E, Banerjee B, Stukenberg PT, Gorbsky GJ, Higgins JM (2010). Histone H3 Thr-3 phosphorylation by Haspin positions Aurora B at centromeres in mitosis. Science 330, 231–235.

Webb DJ, Nuccitelli R (1981). Direct measurement of intracellular pH changes in *Xenopus* eggs at fertilization and cleavage. J Cell Biol 91, 562–567.

Yamagishi Y, Honda T, Tanno Y, Watanabe Y (2010). Two histone marks establish the inner centromere and chromosome bi-orientation. Science 330, 239–243.

Yang HW, Guranovic V, Dutta S, Feng ZK, Berman HM, Westbrook JD (2004). Automated and accurate deposition of structures solved by X-ray diffraction to the Protein Data Bank. Acta Crystallogr D 60, 1833–1839.